AEM
Journals.ASM.org

Carbon Source Preference in Chemosynthetic Hot Spring Communities

Matthew R. Urschel,[a,b] Michael D. Kubo,[c] Tori M. Hoehler,[c] John W. Peters,[b,d] Eric S. Boyd[a,b]

Department of Microbiology and Immunology, Montana State University, Bozeman, Montana, USA[a]; Thermal Biology Institute, Montana State University, Bozeman, Montana, USA[b]; NASA Ames Research Center, Mountain View, California, USA[c]; Department of Chemistry and Biochemistry, Montana State University, Bozeman, Montana, USA[d]

Rates of dissolved inorganic carbon (DIC), formate, and acetate mineralization and/or assimilation were determined in 13 high-temperature (>73°C) hot springs in Yellowstone National Park (YNP), Wyoming, in order to evaluate the relative importance of these substrates in supporting microbial metabolism. While 9 of the hot spring communities exhibited rates of DIC assimilation that were greater than those of formate and acetate assimilation, 2 exhibited rates of formate and/or acetate assimilation that exceeded those of DIC assimilation. Overall rates of DIC, formate, and acetate mineralization and assimilation were positively correlated with spring pH but showed little correlation with temperature. Communities sampled from hot springs with similar geochemistries generally exhibited similar rates of substrate transformation, as well as similar community compositions, as revealed by 16S rRNA gene-tagged sequencing. Amendment of microcosms with small (micromolar) amounts of formate suppressed DIC assimilation in short-term (<45-min) incubations, despite the presence of native DIC concentrations that exceeded those of added formate by 2 to 3 orders of magnitude. The concentration of added formate required to suppress DIC assimilation was similar to the affinity constant (K_m) for formate transformation, as determined by community kinetic assays. These results suggest that dominant chemoautotrophs in high-temperature communities are facultatively autotrophic or mixotrophic, are adapted to fluctuating nutrient availabilities, and are capable of taking advantage of energy-rich organic substrates when they become available.

Life in environments with temperatures that exceed the upper limit of photosynthesis (~73°C) is supported by chemical energy (1–5). In the case of high-temperature (>73°C) terrestrial hot spring environments, the prevalence of members of the bacterial phylum *Aquificales* has been interpreted to reflect the importance of lithoautotrophic metabolism in supporting communities inhabiting these systems (6–11). Cultivated representatives from the order *Aquificales* assimilate dissolved inorganic carbon (DIC) using energy derived from the oxidation of hydrogen (H_2), sulfide (S^{2-}), thiosulfate ($S_2O_3^{2-}$), or elemental sulfur (S_8) under aerobic conditions (7) or H_2, S_8, or $S_2O_3^{2-}$ under anaerobic conditions (12, 13). In addition, some members of the *Aquificales* (i.e., *Thermocrinis* and *Hydrogenobacter* spp.) are facultative autotrophs capable of growing heterotrophically on organic acids or amides, such as formate or formamide, respectively, as their sole carbon and energy source (14, 15).

The presence of organic acids at concentrations capable of supporting the growth of organisms has been reported in many marine and continental hydrothermal environments (e.g., see references 16 and 17), including those in Yellowstone National Park (YNP), Wyoming, where formate was measured at concentrations of up to 10 μM in 56 hot springs (18). The low concentrations of formate in some YNP hot springs (18) may reflect the preferential utilization of this substrate by endogenous populations or a low rate of influx of this substrate into the system. In support of the former possibility, numerous thermophilic organisms capable of growth on formate have been isolated from hot springs (e.g., see references 14 and 19). More direct evidence for the utilization of formate in hot spring communities comes from a [^{13}C]formate-labeling study which documented its incorporation into fatty acids at a single hot spring in YNP, albeit at low levels (20). Indirect evidence for organic acid utilization by hot spring communities comes from a recent study that found 7- to 49-fold increases in the rate of O_2 consumption when microcosms containing sediments sampled from two >73°C springs in the Great Basin of Nevada were amended with an equimolar mixture of formate, lactate, acetate, and propionate, when compared to unamended controls (21). However, it is not clear which of these four organic acids were utilized by the microbial populations in these incubations. Nonetheless, the short incubation time associated with the aforementioned study (<50 min) suggests that the enhanced consumption of O_2 in the presence of organic acids is unlikely to be the result of enrichment of specific populations capable of this activity but, rather, is the result of relative increases in the heterotrophic activity of facultatively autotrophic or heterotrophic populations (21). The dominant populations associated with the sediments used to inoculate the aforementioned microcosms were closely affiliated with the aquificae genus *Thermocrinis*, members of which have been shown to utilize DIC or formate (14, 22).

The energy yield associated with aerobic organic acid oxidation, in particular, formate oxidation, is predicted to be equal to or greater than that derived from the aerobic oxidation of other

Received 12 February 2015 **Accepted** 23 March 2015

Accepted manuscript posted online 27 March 2015

Citation Urschel MR, Kubo MD, Hoehler TM, Peters JW, Boyd ES. 2015. Carbon source preference in chemosynthetic hot spring communities. Appl Environ Microbiol 81:3834–3847. doi:10.1128/AEM.00511-15.

Editor: A. M. Spormann

Address correspondence to Eric S. Boyd, eboyd@montana.edu.

Supplemental material for this article may be found at http://dx.doi.org/10.1128/AEM.00511-15.

doi:10.1128/AEM.00511-15

available reductants (e.g., H_2, H_2S, Fe^{2+}, S_8) under the geochemical conditions that prevail in most hydrothermal systems (18). This indicates that formate may be preferentially metabolized by facultatively autotrophic populations, such as *Thermocrinis* or *Hydrogenobacter* spp., when it is available. Consistent with this hypothesis, carbon isotopic analysis of membrane lipids extracted from pink streamer communities sampled from Octopus Spring (OS; 84 to 88°C), YNP, Wyoming, shown previously to be dominated by 16S rRNA gene sequences affiliated with *Thermocrinis* (23), showed that they were depleted in ^{13}C relative to the amount of DIC in hydrothermal fluids sampled from the spring's source (24). On the basis of a comparison of these membrane lipid carbon isotope signatures with those obtained from cultures of *Thermocrinis ruber* (originally isolated from OS [14]) grown autotrophically with H_2 or heterotrophically with formate, it was concluded that the *Thermocrinis* organisms inhabiting OS were most likely growing heterotrophically and may have been metabolizing formate (24). Likewise, a recent compound-specific analysis of aquificae lipid biomarkers recovered from filamentous communities inhabiting OS revealed carbon isotopic compositions that were more similar to those of the dissolved organic carbon (DOC) pool than to those of the DIC pool. This finding was interpreted to reflect a predominantly heterotrophic lifestyle of these organisms (25). In contrast, the carbon isotopic compositions of these same aquificae-specific lipids recovered from sediments or filaments collected from Flat Cone (74°C) and "Bison Pool" (BP; 74 to 86°C; unofficial feature names are denoted with quotation marks), YNP, revealed values that were more similar to those for DIC present in spring waters, indicating a predominantly autotrophic lifestyle. Previous studies have shown that filament- or sediment-associated communities obtained from the source vents of Flat Cone (E. S. Boyd, unpublished data) and "Bison Pool" (8) are dominated by aquificae closely affiliated with *Thermocrinis* spp. Taken together, such observations may allude to the importance of the intermittent surface input of organic carbon into these systems from precipitation runoff, aeolian deposition, or other exogenous sources. The exogenous input of organic carbon by any of these mechanisms could initiate a shift in the metabolism of facultatively autotrophic aquificae toward heterotrophy in order to maximize energy conservation.

In the present study, we compared rates of C assimilation or mineralization from DIC (CO_2 plus bicarbonate), formate, and acetate in 13 chemotrophic communities that span large geochemical gradients in YNP to evaluate the hypothesis that nonphototrophic microbial communities inhabiting high-temperature (>73°C) hot springs are supported primarily by the autotrophic assimilation of inorganic carbon. To determine carbon source preference, we evaluated the extent to which amendment with low (micromolar) levels of formate suppresses DIC assimilation. These data were combined with the results of taxonomic profiling of archaeal and bacterial 16S rRNA gene sequences and geochemical measurements in order to identify (i) populations putatively involved in substrate transformations and (ii) geochemical regimes that may influence potential rates of substrate transformation.

MATERIALS AND METHODS

Physical and chemical measurements. Samples used for chemical and biological measurements were collected between July and October 2012. The pH of hot spring fluids was measured on-site with a YSI pH100CC-01 pH meter. Conductivity and temperature were measured using a YSI EC300 conductivity meter (YSI, Inc., USA). Ferrous iron (Fe^{2+}) and total sulfide (S^{2-}) were quantified using Hach ferrozine pillows and Hach sulfide reagents 1 and 2, respectively, and a Hach DR/890 spectrophotometer (Hach Company, Loveland, CO). Dissolved nitrate (NO_3^-), nitrite (NO_2^-), and total ammonia [$NH_4(T)$] were determined with AccuVac ampoules for nitrate or nitrite and an AmVer ammonia reagent set for total ammonia (Hach Company). $NH_4(T)$ refers to the sum of the dissolved species of aqueous NH_3 and NH_4^+, as measured by colorimetry (26). For organic acid analyses, 10 ml of spring water was filtered through 0.2-μm-pore-size polyethersulfone syringe filters into precombusted glass vials with polytetrafluoroethylene-lined silicone septa. The vials were frozen and stored at −20°C until analysis via high-performance liquid chromatography using a previously described alternate injection procedure (27). For determination of DIC, hot spring water was filtered (pore size, 0.2 μm) and frozen at −20°C prior to acidification and quantification via a gas chromatograph, as previously described (28).

Microcosm preparation. Rates of DIC, formate, and acetate assimilation and mineralization were quantified using a previously described microcosm-based approach (4, 11). Microcosms were prepared in presterilized 24-ml serum bottles. Roughly 100 mg of sediment was added to each vial, and the bottle was capped with a butyl rubber stopper and purged with N_2 for ~5 min. Sediments were overlaid with 10 ml of spring water sampled directly from the spring using a syringe and needle. The gas phase of all microcosms was equalized to atmospheric pressure using a sterile needle prior to injection of 10.0 μCi (final concentration, 20 μM) of [^{14}C]sodium bicarbonate ($NaH^{14}CO_3$) for DIC assays, 7.5 μCi (final concentration, 14.4 μM) of [^{14}C]sodium formate ($H^{14}COONa$) for formate assays, and 5 μCi (final concentration, 9.4 μM) of 1-[^{14}C]sodium acetate ($CH_3{}^{14}COONa$) or 5 μCi (final concentration, 8.9 μM) of 2-[^{14}C]sodium acetate ($^{14}CH_3COONa$) for acetate assays. Data from individual 1-[^{14}C]- and 2-[^{14}C]acetate assays were combined to quantify the rate of acetate assimilation or mineralization.

All microcosms were wrapped in aluminum foil to eliminate light, placed in a sealed bag (secondary containment), and incubated in the source of the spring for ~30 to 45 min. Triplicate microcosms for each assay condition were terminated by freezing on dry ice and were stored at −20°C until processed (described below). The authors acknowledge that it is not possible to precisely mimic the natural hydrological conditions in a geothermal spring using a microcosm-based approach. However, the rapid addition of sediment and fluids taken directly from each spring, along with the short incubation times (30 to 45 min) used in these experiments, was aimed at minimizing variation between microcosm conditions and actual spring conditions that could potentially arise from outgassing, contact with atmospheric gases, and/or nutrient limitation in a closed system. Our previous findings support the effectiveness of this approach to minimize the bottle effect, as the rates of CO_2 fixation associated with a thermoacidophilic community in a continuous-flow reactor system were shown to be statistically indistinguishable from those associated with a thermoacidophilic community from the same spring location in short-term (<2-h) microcosm incubations (11).

Assays were developed to investigate the response of DIC assimilation to amendment with formate in select hot spring ecosystems. Microcosms were prepared in triplicate as described above using $NaH^{14}CO_3$ as the radiotracer for DIC assimilation. Microcosms were then amended with 0, 5, 10, or 20 μM unlabeled formate, incubated for 45 min, and quenched by freezing as described above. Assays for suppression of DIC assimilation were carried out in "Dragon Spring" (DS), Cinder Pool (CP), Evening Primrose (EP), Perpetual Spouter (PS), and BP in order to capture a subset of the geochemical regimes selected for examination in this study.

Microcosm assays were conducted to determine the affinity constant (K_m; the concentration at which the formate conversion velocity reaches one-half of its maximum rate) for chemosynthetic microbial communities in the same 5 YNP hot springs in which substrate suppression assays were carried out. A 10 mM [^{12}C]sodium formate ($H^{12}COONa$) stock solution that contained 50 μCi (0.96 μmol) of radiolabeled formate

($H^{14}COONa$) as a tracer was prepared. Microcosms were prepared with final formate concentrations (i.e., [^{12}C]formate plus [^{14}C]formate) of 1.25, 2.50, 5.00, or 10.0 μM. Microcosms were prepared, incubated, and analyzed for formate conversion activity as described below. To determine formate conversion rates, the rate at which CO_2 was produced from formate oxidation (the methods are described below) was combined with the rate of C assimilation from formate. The equations of Wright and Hobbie (29) were used to determine the K_m of formate conversion because they allow the calculation of kinetic parameters at low substrate concentrations (e.g., <20 μM) and when the natural substrate concentration is not known, as was the case in many of the springs analyzed (see Table 2).

Determination of ^{14}C in microcosm headspace or filtered biomass. In the laboratory, sealed microcosm assay mixtures were thawed at room temperature for approximately 2 h, followed by acidification to a pH of ~2.0 by injection of 1.0 ml of 1 N HCl into the headspace to volatize unreacted CO_2 and to protonate organic acids, thereby minimizing adsorption through electrostatic interactions. After acidification, the microcosms were allowed to equilibrate for an additional 2 h. To estimate formate and acetate mineralization rates, N_2-purged serum bottles (12 ml) containing 1 ml of the CO_2-absorbing solution Carbo-Sorb E (PerkinElmer, Inc., Santa Clara, CA, USA) were prepared. The gas phase in the Carbo-Sorb E serum bottles was removed by vacuum so that it was −10 torr, and 5 ml of the gas phase from each microcosm (sampled using a 10-ml syringe and stopcock) was injected into the bottle containing the Carbo-Sorb E solution. The potential for confounding effects due to the development of a partial vacuum upon removal of the gas phase in microcosms could not be accounted for in the experimental design. Carbo-Sorb E was allowed to react with the sampled gas at room temperature (~22°C) for approximately 2 h. Following incubation, the vials were opened and the Carbo-Sorb E solution was removed with a 1-ml pipette and discharged into 10 ml of CytoScint ES liquid scintillation fluid (MP Biomedicals, USA) for use in liquid scintillation counting (LSC), as described below.

To determine the amount of ^{14}C assimilated into biomass from DIC, formate, and acetate, acidified samples were filtered onto 0.22-μm-pore-size polycarbonate membranes. Filtered samples were washed with 5 ml of sterile deionized water, dried overnight at 80°C, and weighed to determine the number of grams (dry mass) (gdm) of the filtrate. Dried filters were placed in scintillation vials and overlaid with 10 ml of CytoScint ES liquid scintillation fluid. The radioactivity associated with each of the samples (Carbo-Sorb E solution and filtered sediment) was measured on a Beckman LS 6500 liquid scintillation counter (Beckman Coulter, Inc., Indianapolis, IN). The rates of C assimilation and mineralization were determined on the basis of the results obtained with the ^{14}C tracers using the methods of Lizotte et al. (30). Briefly, uptake rates were calculated by multiplying the uptake of ^{14}C-labeled substrate by the total effective concentration of the substrate (the concentration of ^{14}C-labeled substrate plus the concentration of native substrate). In cases where the concentration of native formate or acetate was below the detection limit, a concentration corresponding to the detection limit was used. Thus, rates of formate or acetate assimilation and mineralization may be overestimated in these systems and may be more appropriately considered rate potentials (see Discussion) rather than absolute rates. Recognizing that isotopic discrimination factors differ for different autotrophic processes (as summarized by Havig et al. [31]) and are likely to differ for different modes of formate and acetate metabolism, we adopted the uniform isotopic discrimination factor of 1.06, as described previously (30). The data derived from 1-[^{14}C]acetate and 2-[^{14}C]acetate assays were combined prior to calculation of the overall rates of acetate assimilation and mineralization. The mean and standard deviation of the rates of substrate transformation normalized to the number of grams (dry mass) per hour are presented.

Sequencing of bacterial and archaeal 16S rRNA genes. Genomic DNA was extracted in duplicate from ~250 mg of hot spring sediment as previously described (32). Equal volumes of replicate extractions were pooled and quantified using a Qubit DNA assay (Life Technologies, Grand Island, NY) and a Qubit (version 2.0) fluorometer (Life Technologies). Thirty-five cycles of PCR were conducted using either bacterium-specific primers (1100F/1492R) or archaeon-specific primers (344F/915R) and the reaction and cycling conditions previously described (33). PCR products were purified using a Promega Wizard PCR purification system (Madison, WI) and were quantified via the Qubit DNA assay as described above. Amplicons were submitted to MrDNA (Shallowater, TX) for bar coding and multiplex sequencing by use of the 454 Titanium sequencing platform (Roche, Indianapolis, IN). Postsequencing processing was performed with mothur (version 1.25.1) software (34), as previously described (33), after removing reads of less than 225 bp. Raw untrimmed sequence and quality score files along with a mapping file have been deposited in the NCBI SRA database under accession number SRR1042042.

Phylogenetic analysis of archaeal and bacterial 16S rRNA genes for each operational taxonomic unit (OTU) was performed by the use of approximate likelihood ratio tests (35) implemented in the PhyML (version 3.0) program (35). Bacterial 16S rRNA gene phylogenies were rooted with small-subunit (SSU) rRNA genes from *Acidilobus sulfurireducens* strain 18D70 (GenBank accession number EF057391) and *Caldisphaera draconis* strain 18U65 (GenBank accession number EF057392). Archaeal 16S rRNA gene phylogenies were rooted with SSU rRNA genes from *Clostridium acetobutylicum* ATCC 824 (GenBank accession number AE001437) and *Caldicellulosiruptor saccharolyticus* DSM 8903 (GenBank accession number CP000679). Phylogenies were constructed using the general time-reversible (GTR) substitution model with a proportion of invariable sites and gamma-distributed rate variation, as recommended by the ModelTest (version 3.8) program (36). Phylograms were rate smoothed using the multidimensional version of Rambaut's parameterization, as implemented in the PAUP (version 4.0) program (37). Rate smoothing for each phylogram was performed according to the parameters identified using ModelTest. This included the identification of the substitution model, the gamma distribution of the rate variation across sites, the proportion of invariant sites, nucleobase frequencies, and the rate matrix for each phylogram. The rate-smoothed cladograms were used to construct phylogenetic distance matrices for each cladogram with the program Phylocom (version 4.0.1) (38).

Statistical analyses. For the purposes of statistical analysis, all environmental measurements that were below the limit of detection were assigned a value equal to the detection limit for that particular measurement (see Table 1). The relationships between the measured DIC, formate, and acetate transformation rates and the geochemical variables for each of the hot spring environments were evaluated using a multivariate ordination method known as redundancy analysis (RDA). RDA was performed with the Vegan (version 2.0.3) program (http://vegan.r-forge.r-project.org/) implemented within the R statistical computing package (version 2.15.0). All rate measurements were log(base 10) transformed prior to analysis in order to preserve overall trends as a function of geochemical measurements and to allow visualization of DIC assimilation data alongside formate and acetate assimilation data, despite differences in these measurements of as large as 1 order of magnitude. RDA plots were scaled symmetrically by taking the square root of eigenvalues for both vectors. Cluster analysis was also used to visualize patterns in the cumulative rates of DIC, formate, and acetate mineralization and/or assimilation. The PAST (version 1.72) program (39) was used to generate cluster dendrograms specifying paired linkage and Bray-Curtis distances. Bootstrap values correspond to the frequency of observation for each node in a given position out of 100 replicates. Principle coordinates (PCO) analysis was used to visually identify patterns of community clustering using the Rao phylogenetic distance matrix. PCO ordination and cluster analyses were performed using the Vegan program implemented in R (version 2.10.1).

TABLE 1 Location and field measurements for YNP hot springs sampled in this study

pH group and YNP thermal inventory identifier	Spring name[a]	Spring abbreviation	Thermal area[b]	Global Positioning System coordinates	Conductivity (mS)	Temp (°C)	pH
Acidic (pH <4.0)							
GSSG060	"Lobster Claw"	A(LC)	SS	44°41′58.00″N, 110°46′05.70″W	7.1	85.2	1.9
CHA043	"Alice Spring"	A(AS)	CH	44°39′11.82″N, 110°2′05.06″W	5.3	77.5	2.3
NHSP106	"Dragon Spring"	A(DS)	NGB	44°4′54.60″N, 110°4′39.20″W	3.3	78.0	2.5
Moderately to slightly acidic (pH 4.0–6.9)							
NHSP103	Cinder Pool	MA(CP)	NGB	44°4′56.89″N, 110°4′35.40″W	5.0	88.7	4.0
NA[c]	"Hell's Gate"	MA(HG)	RC	44°3′31.44″N, 110°4′32.46″W	0.4	88.0	4.4
GSSG038	Evening Primrose	MA(EP)	SS	44°4′57.70″N, 110°4′01.80″W	4.8	78.4	5.1
MV007	Obsidian Pool	MA(OP)	MV	44°3′36.50″N, 110°2′19.50″W	0.2	74.5	5.4
NA	"Corner Thing"	MA(CT)	GC	44°4′26.52″N, 110°4′46.50″W	0.2	85.8	5.9
Neutral to alkaline (pH >7.0)							
NBB113	Perpetual Spouter	NA(PS)	NGB	44°4′35.80″N, 110°4′32.80″W	6.0	84.3	7.1
LSMG013	"Bison Pool"	NA(BP)	SM	44°3′10.67″N, 110°5′54.65″W	3.2	80.0	7.8
NA	"Rabbit Creek South"	NA(RCS)	RC	44°3′31.74″N, 110°4′32.46″W	0.5	88.3	8.2
LSMG004	Flat Cone	NA(FC)	SM	44°3′06.59″N, 110°5′48.70″W	1.6	77.1	8.2
NA	"Rabbit Creek North"	NA(RCN)	RC	44°3′11.40″N, 110°4′38.88″W	2.1	88.6	9.2

[a] Several of the features sampled do not have official YNP names. Unofficial names are denoted with quotation marks.
[b] NGB, Norris Geyser Basin; CH, Crater Hills; GC, Geyser Creek; MV, Mud Volcano; RC, Rabbit Creek; SM, Sentinel Meadows; SS, Sylvan Springs.
[c] NA, not available.

RESULTS

Overview of hot spring sampling sites. The 13 geothermal springs selected for analysis were located in one of seven distinct thermal areas in YNP, which included Norris Geyser Basin (NGB), Crater Hills (CH), Geyser Creek (GC), Mud Volcano (MV), Rabbit Creek (RC), Sentinel Meadows (SM), and Sylvan Spring (SS) (Tables 1 and 2; see also Fig. S1 and S2 in the supplemental material). For the purposes of this study, we organized experimental field sites into three groups on the basis of the spring pH: acidic (pH <4.0), moderately to slightly acidic (pH 4.0 to 6.9), and neutral to alkaline (pH >6.9), which are represented by the prefixes A, MA, and NA, respectively, followed by the spring name abbreviation in parentheses (Tables 1 and 2). The A group includes the three low-pH springs "Lobster Claw" [A(LC)], "Dragon Spring" [A(DS)], and "Alice Spring" [A(AS)]. These springs are characterized as having elevated sulfide, ferrous iron, and total ammonia concentrations (Table 1). The MA group included Cinder Pool [MA(CP)], "Hell's Gate" [MA(HG)], Evening Primrose [MA(EP)], Obsidian Pool [MA(OP)], and "Corner Thing" [MA(CT)]. These springs were characterized by moderate concentrations of sulfide and total ammonia. Springs in both the A and MA groups often contained deposits of solid-phase S_8 [A(DS), MA(CP), MA(EP)] or iron oxides [A(LC), MA(HG), MA(CT)] or were clay rich [A(LC), A(AS), MA(CP), MA(EP)] (see Fig. S1 in the supplemental material). The NA group

TABLE 2 Concentrations of DIC, organic acids, and selected ions in source waters sampled from 13 YNP hot springs

pH group and site	DIC concn (mM)	Concn[a] (μM)						
		Formate	Acetate	S_2^{2-}	Fe^{2+}	NH_4(T)	NO_2^-	NO_3^-
Acidic (pH <4.0)								
A(LC)	0.7	1.6	BD (0.8)	14.0	7.2	261.3	BD (0.1)	1.6
A(AS)	37.1	26.6	20.2	BD (0.3)	207.7	552.0	BD (0.1)	BD (0.2)
A(DS)	0.3	0.8	BD (0.8)	24.9	21.8	67.5	0.8	43.5
Moderately to slightly acidic (pH 4.0–6.9)								
MA(CP)	1.2	BD (0.1)	BD (0.8)	6.2	4.7	392.2	BD (0.1)	9.7
MA(HG)	0.1	0.8	BD (0.8)	3.7	9.7	134.5	2.5	BD (0.2)
MA(EP)	2.4	BD (0.1)	BD (0.8)	BD (0.3)	1.4	66.4	BD (0.1)	BD (0.2)
MA(OP)	1.0	0.2	BD (0.8)	0.3	3.2	6.5	BD (0.1)	BD (0.2)
MA(CT)	1.7	BD (0.1)	BD (0.8)	5.3	1.6	28.2	BD (0.1)	29.0
Neutral to alkaline (pH >7.0)								
NA(PS)	0.1	BD (0.1)	BD (0.8)	1.6	1.2	15.3	BD (0.1)	BD (0.2)
NA(BP)	6.0	BD (0.1)	BD (0.8)	BD (0.3)	BD (1.0)	BD (1.2)	BD (0.1)	19.4
NA(RCS)	2.8	0.9	2.0	BD (0.3)	BD (1.0)	5.9	16.4	BD (0.2)
NA(FC)	4.9	BD (0.1)	BD (0.8)	11.8	BD (1.0)	BD (1.2)	BD (0.1)	27.4
NA(RCN)	2.8	1.3	2.1	16.2	BD (1.0)	10.0	5.4	38.7

[a] BD, below the detection limit (the detection limit is given in parentheses).

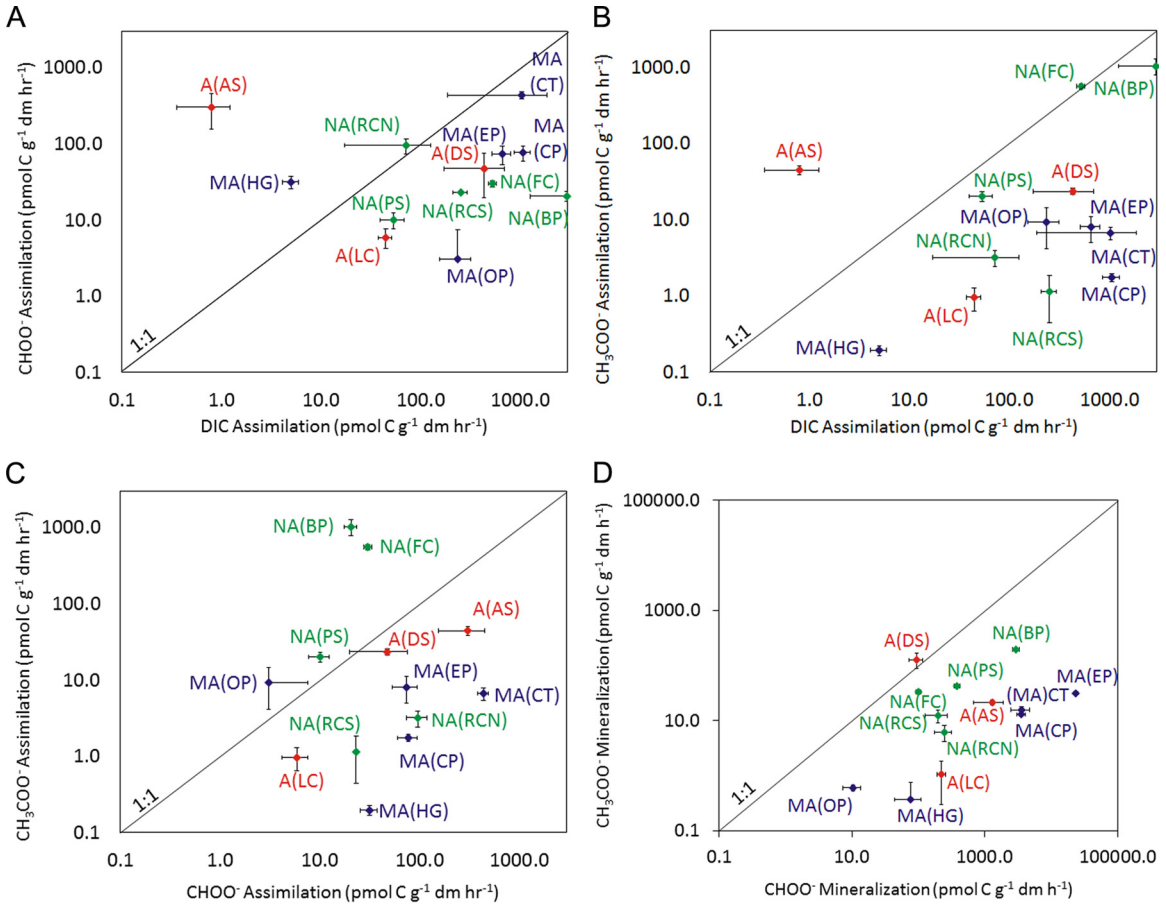

FIG 1 Rates of C assimilation or mineralization from DIC, formate, and acetate in microbial communities sampled from the sources of 13 YNP hot springs. Site labels correspond to those presented in Tables 1 and 2. The 1:1 lines are presented to facilitate comparison of the rates of substrate transformation. The rates of individual substrate transformation for each assemblage are reported in Table S1 in the supplemental material. Red, acidic springs (pH <4.0); navy blue, moderately acidic springs (pH 4.0 to 6.9); green, neutral to alkaline springs (pH >7.0).

consists of Perpetual Spouter [NA(PS)], "Bison Pool" [NA(BP)], "Rabbit Creek South" [NA(RCS)], Flat Cone [NA(FC)] and "Rabbit Creek North" [NA(RCN)]. These springs tended to have low concentrations of ferrous iron and total ammonia compared to those in the other groups and at the time of sampling did not have visual deposits of iron or sulfur (see Fig. S1 in the supplemental material).

Rates of carbon transformation by chemotrophic communities. DIC, formate, and acetate assimilation or mineralization was detected in all 13 hot spring communities examined in this study (Fig. 1; see also Table S1 in the supplemental material). The rate of C assimilation from DIC exceeded that of C assimilation from formate (Fig. 1A) in 9 of the 13 communities examined. Similarly, the rate of C assimilation from DIC exceeded the rate of C assimilation from acetate in 11 of the 13 communities examined (Fig. 1B). Assimilation of C from either formate or acetate was detected in all 13 of the hot spring communities analyzed (Fig. 1C), with the rate of C assimilation from formate being greater than that from acetate in 8 of the 13 hot spring communities. Mineralization of C from either formate or acetate was also detected in all 13 springs examined (Fig. 1D), with the rate of formate mineralization exceeding that of acetate mineralization in 12 of the communities. Importantly, the data presented here were normalized to the number of moles of C assimilated from DIC, formate, or acetate. A true comparison of the turnover of DIC and formate molecules relative to that of acetate molecules requires that the rate of C assimilation or mineralization from acetate be divided by two (2 C atoms per mole of acetate). Application of this conversion factor reveals that acetate turnover was greater than DIC turnover in only 1 of the springs examined, while acetate turnover exceeded formate turnover in 2 of the springs examined.

Cluster analysis was performed to elucidate patterns in the cumulative rates (the rates for DIC, formate, and acetate combined) of C assimilation and mineralization (Fig. 2A). Cumulative substrate transformation activities in the 13 hot spring communities clustered primarily due to variation in temperature and pH. For example, rates of DIC, formate, and acetate transformation were similar in NA(RCS) (88.3°C, pH 8.2) and NA(RCN) (88.6°C, pH 9.2). RDA revealed similar patterns of clustering and further allowed the elucidation of patterns in the cumulative rates (the rates for DIC, formate, and acetate combined) of C transformation in relation to the individual rates of assimilation and mineralization from DIC, formate, and acetate, as well as hot spring geochemistry (Fig. 2B). The centroid of the RDA ordination plot represents the average cumulative rate of C assimilation and mineralization for the combined 13 hot spring communities. For example, the cumulative assimilation rate for the NA(RCN) and NA(RCS) com-

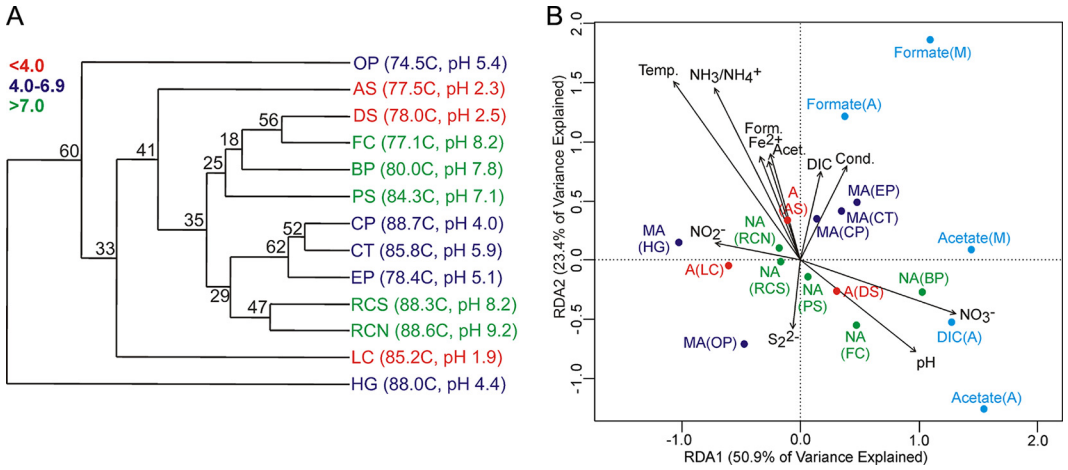

FIG 2 (A) Paired-group cluster analysis depicting the Bray-Curtis similarity in cumulative rates of C assimilation and mineralization from DIC, formate, and acetate in 13 YNP hydrothermal communities. The temperature and pH of the springs are indicated. Spring labels are color coded on the basis of similarity in spring pH. The cophenetic correlation coefficient for the reconstructed dendrogram was 0.89, indicating a good fit of the 2-dimensional model to the data. (B) RDA ordination of the cumulative rates of C assimilation and mineralization from DIC, formate, and acetate in 13 hot spring communities. The cumulative activities for communities were ordinated, and their positions in relation to the individual rates of substrate transformation (light blue) are indicated. The plot was overlaid with measured geochemical variables (black), with the direction of the vectors indicating the relationship to cumulative and individual rates of substrate transformation. Site labels correspond with those in Tables 1 and 2. Temp., temperature; Form., formate; Acet., acetate; Cond., conductivity. Red, acidic springs (pH <4.0); navy blue, moderately acidic springs (pH 4.0 to 6.9); green, neutral to alkaline springs (pH >7.0).

munities was close to the average value for all communities examined, as exhibited by the clustering of this site near the centroid. Hot spring communities that plot away from the centroid exhibit a rate(s) of C assimilation or mineralization from DIC, formate, and/or acetate that deviates from the average. The first two RDA axes explained 74.3% of the cumulative variation in the measured rates, with RDA axis 1 accounting for 50.9% of the total variance and RDA axis 2 accounting for 23.4% of the variance. Regression analysis indicates that RDA axis 1 was positively correlated with the rate of C assimilation from DIC (Pearson $R = 0.68$, $P = 0.01$), C assimilation and mineralization from acetate (Pearson $R = 0.80$ and 0.90, respectively; $P = 0.01$ and $P < 0.01$, respectively), and C mineralization from formate (Pearson $R = 0.58$, $P = 0.03$) (see Table S2 in the supplemental material). In contrast, RDA axis 2 was positively correlated with the rate of C assimilation and mineralization from formate (Pearson $R = 0.73$ and 0.76, respectively; $P < 0.01$ and $P < 0.01$, respectively). Thus, RDA axis 1 is separating communities primarily on the basis of differences in the rates of DIC and acetate metabolism and, to a lesser extent, formate metabolism. In contrast, RDA axis 2 is separating communities primarily on the basis of differences in the rates of formate metabolism.

Similar to the results of the cluster analysis described above, RDA indicated that the rates of C assimilation and mineralization in communities residing in hot springs with similar geochemical conditions often formed clusters. For example, the cumulative rates of C assimilation and mineralization in MA(CT) and MA(CP), both of which are high-temperature hot springs with a slightly acidic pH, formed a cluster near the centroid of the RDA plot. This cluster was oriented along the individual vectors associated with the rates of C assimilation and mineralization from formate. The cumulative rates of C assimilation and mineralization in NA(FC), NA(PS), A(DS), and NA(BP) also formed a cluster that trended in the direction of vectors describing the individual rates of C assimilation from DIC and acetate as well as acetate mineralization.

An overlay of measured geochemical variables reveals that C assimilation and mineralization from DIC, acetate, and, to a lesser extent, formate are positively correlated with pH over the range of pHs of the hot springs studied (1.9 to 9.2). This indicates that the rates of transformation of these substrates are, on average, greater in systems with circumneutral to alkaline pHs [e.g., NA(PS), NA(BP)] than in moderately acidic to acidic systems [e.g., A(AS), MA(CT)]. The rates of C assimilation and mineralization from DIC and acetate were inversely correlated with temperature, whereas the rates of C assimilation and mineralization from formate were positively correlated with temperature.

Rates of assimilation and mineralization of 1-[^{14}C]- and 2-[^{14}C]acetate. Separate microcosm assays were conducted for acetate labeled singly at the carboxyl position (1-[^{14}C]acetate) or singly at the methyl position (2-[^{14}C]acetate) (see Table S3 in the supplemental material), thus allowing a comparison of the rates of assimilation and mineralization at these positions (Fig. 3). For labeling at the carboxy position, rates of mineralization were greater than those of assimilation in 3 of the 13 communities analyzed, less than those of assimilation in 8 of the communities, and not significantly different from those of assimilation in 2 of the communities. For labeling at the methyl position, the rates of mineralization were greater than those of assimilation in 7 of the 13 communities analyzed, less than those of assimilation in 2 of the communities, and not significantly different from those of assimilation in 4 of the communities. A comparison of the rate of assimilation from the carboxyl and methyl carbons of acetate indicated that the carboxyl carbon was preferentially assimilated in 3 communities, while the methyl carbon was preferentially assimilated in 3 communities; 7 of the communities did not exhibit significant differences in assimilation of the carboxyl or methyl carbon of acetate. The carboxyl carbon was preferentially miner-

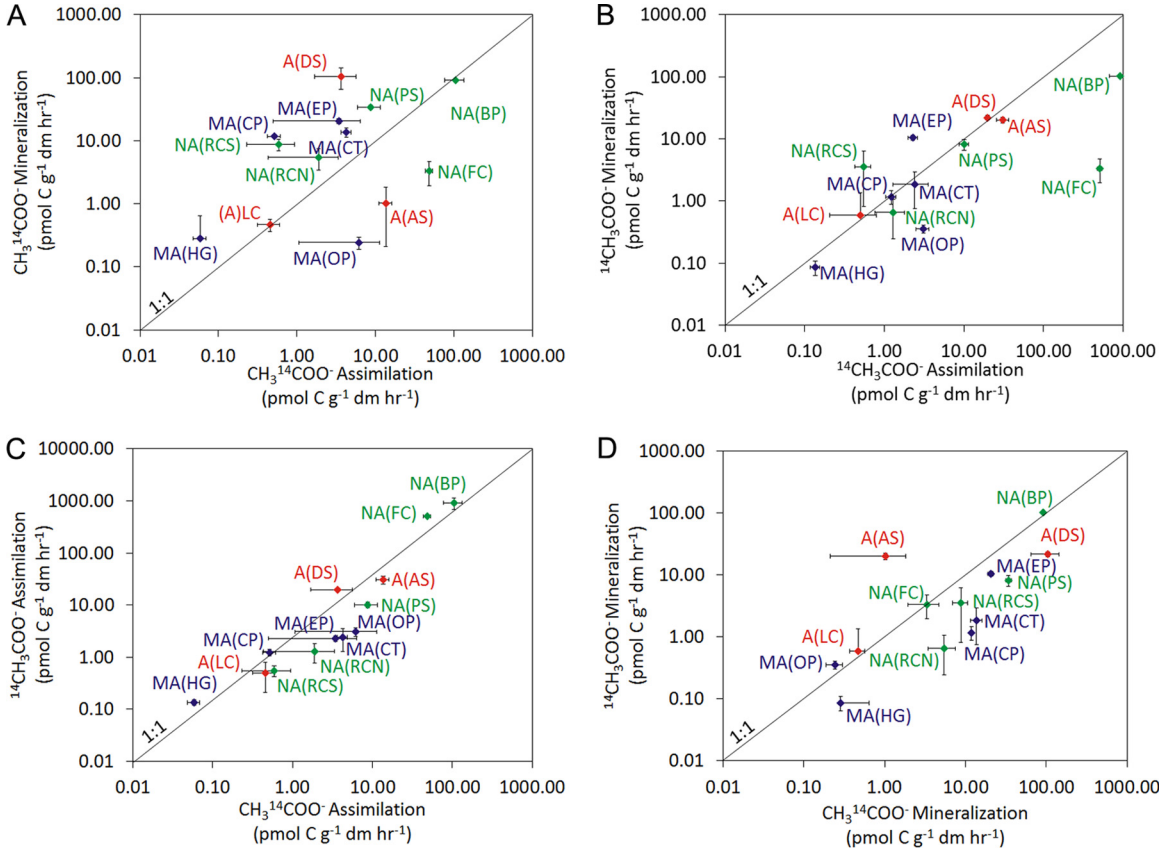

FIG 3 Rate of C assimilation or mineralization from $CH_3{}^{14}COO^-$ (1-[^{14}C]acetate) and $^{14}CH_3COO^-$ (2-[^{14}C]acetate) in microbial communities sampled from the sources of 13 YNP hot springs. Site labels correspond to those presented in Table 1. Red, acidic springs (pH <4.0); navy blue, moderately acidic springs (pH 4.0 to 6.9); green, neutral to alkaline springs (pH >7.0). The 1:1 lines are presented to facilitate comparison of the rates of substrate transformation. The rates of individual substrate transformation for each assemblage are reported in Table S3 in the supplemental material.

alized in 8 communities, while the methyl carbon was preferentially mineralized in 4 communities; 1 community did not exhibit a significant difference in mineralization of the carboxyl or methyl carbon of acetate.

Suppression of DIC assimilation by formate. A series of microcosm experiments was conducted to investigate whether hot spring populations are capable of simultaneous utilization of CO_2 and formate or are capable of shifting their metabolism from CO_2 assimilation to formate uptake in order to take advantage of formate as it becomes available in their environment. The amount of ^{14}C incorporated into biomass was monitored in microcosms amended with increasing concentrations of unlabeled formate for five hot springs [A(DS), MA(CP), MA(EP), NA(PS), and NA(BP)]. These springs were selected as their pHs span the full range of pHs represented among the 13 sites examined and to target sites in which both DIC and formate metabolism had been detected. In all five springs, assimilation of DIC was systematically suppressed by amendment with increasing concentrations of formate (Fig. 4). The concentration of formate required to suppress DIC assimilation to a level that was significantly lower than that of the unamended control varied among the hot spring communities analyzed. Whereas 5 μM formate was required to significantly (Student *t* test, $P < 0.05$) suppress DIC assimilation relative to the level of DIC assimilation for the unamended controls in the A(DS), NA(BP), and NA(PS) communities, a similar response was not observed in the MA(EP) and MA(CP) communities until 10 and 20 μM formate, respectively, was added. In addition to the observed difference in the formate concentration required to significantly suppress DIC assimilation, the magnitude of the suppression response induced by formate amendment (5, 10, and 20 μM) also differed between the microbial assemblages.

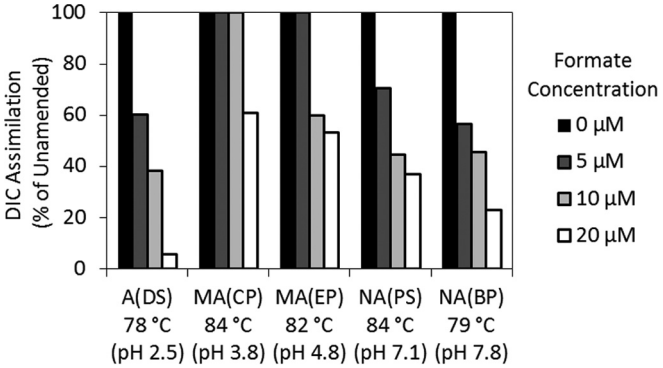

FIG 4 Suppression of DIC assimilation by amendment with various concentrations of formate in microbial communities sampled from the sources of five YNP hot springs. DIC assimilation is depicted as a percentage of that for the unamended (0 μM formate) controls. Site labels correspond to those presented in Tables 1 and 2.

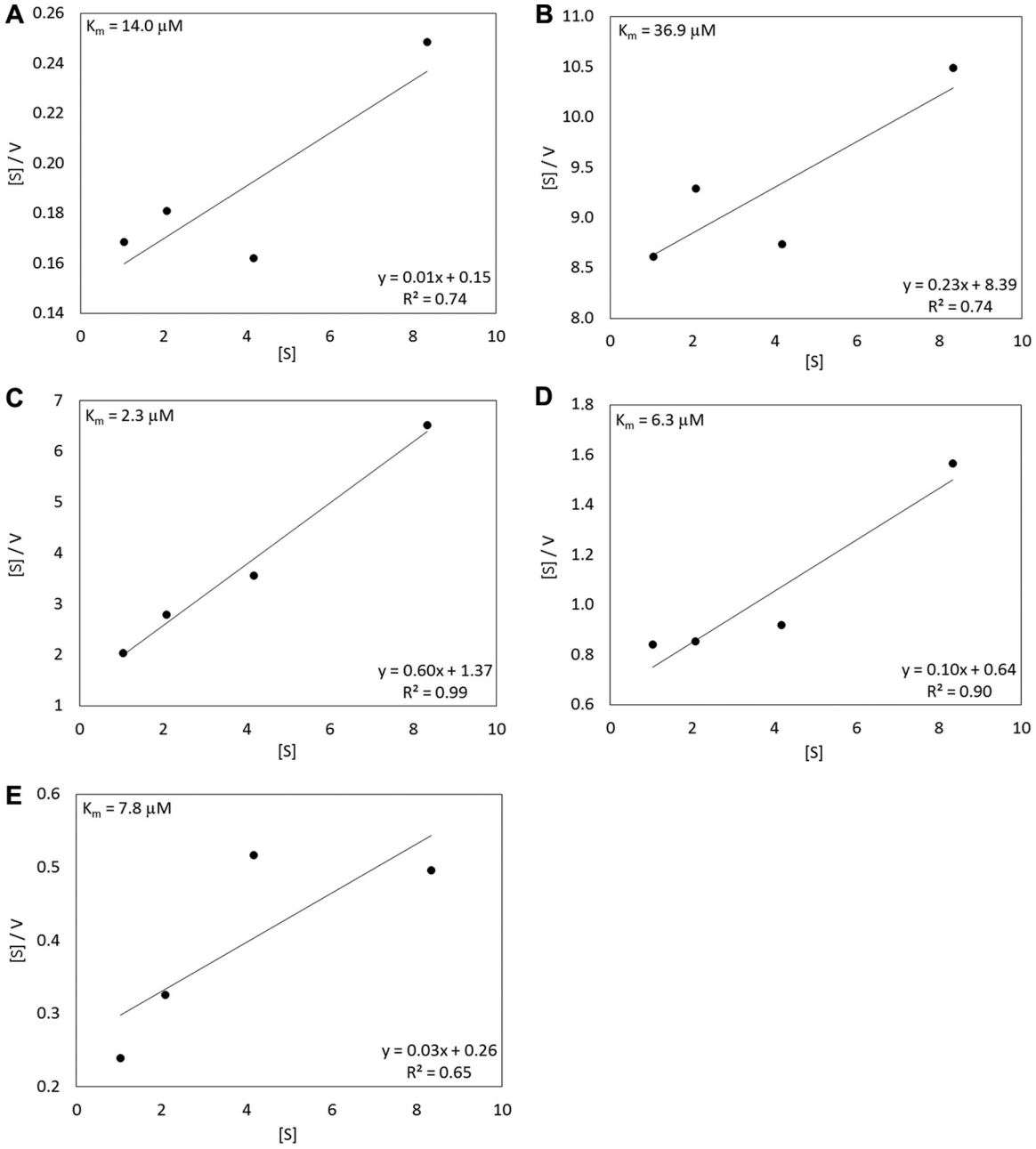

FIG 5 Results of formate kinetic assays in 5 select YNP geothermal features. The equations of Wright and Hobbie (29) were used to determine affinity constants (K_m values). The calculated K_m values for "Bison Pool" (A), Cinder Pool (B), "Dragon Spring" (C), Evening Primrose (D), and Perpetual Spouter (E) are presented. [S], substrate concentration; V, velocity.

Formate transformation kinetics. Community kinetic assays were conducted to estimate the affinity for formate in the 5 communities where DIC suppression assays were conducted (Fig. 5). To avoid the potential confounding effects of formate toxicity at concentrations above 100 μM (see Discussion), we amended the assay mixtures with <20 μM formate. Plots obtained by use of the equations of Wright and Hobbie (29) indicated community formate uptake affinities (K_m values) of 14.0, 36.9, 2.3, 6.3, and 7.8 μM in NA(BP), MA(CP), A(DS), MA(EP), and NA(PS), respectively (Fig. 5). These values were broadly similar to the concentrations of formate required to significantly suppress the DIC assimilation rate in the same communities (Fig. 4). Importantly, the kinetic values reported here should be regarded as conservative estimates, since the rate data used for kinetic determination were normalized to the number of grams (dry mass) of sediments rather than a measurement of biomass and the communities may comprise more than one formate-utilizing organism.

Archaeal and bacterial 16S rRNA gene composition. The taxonomic composition of bacterial and archaeal assemblages in the 13 hot springs was examined in order to identify putative taxa responsible for the measured C transformation activities (Fig. 6A and B). Bacterial amplicons were obtained from sediment DNA

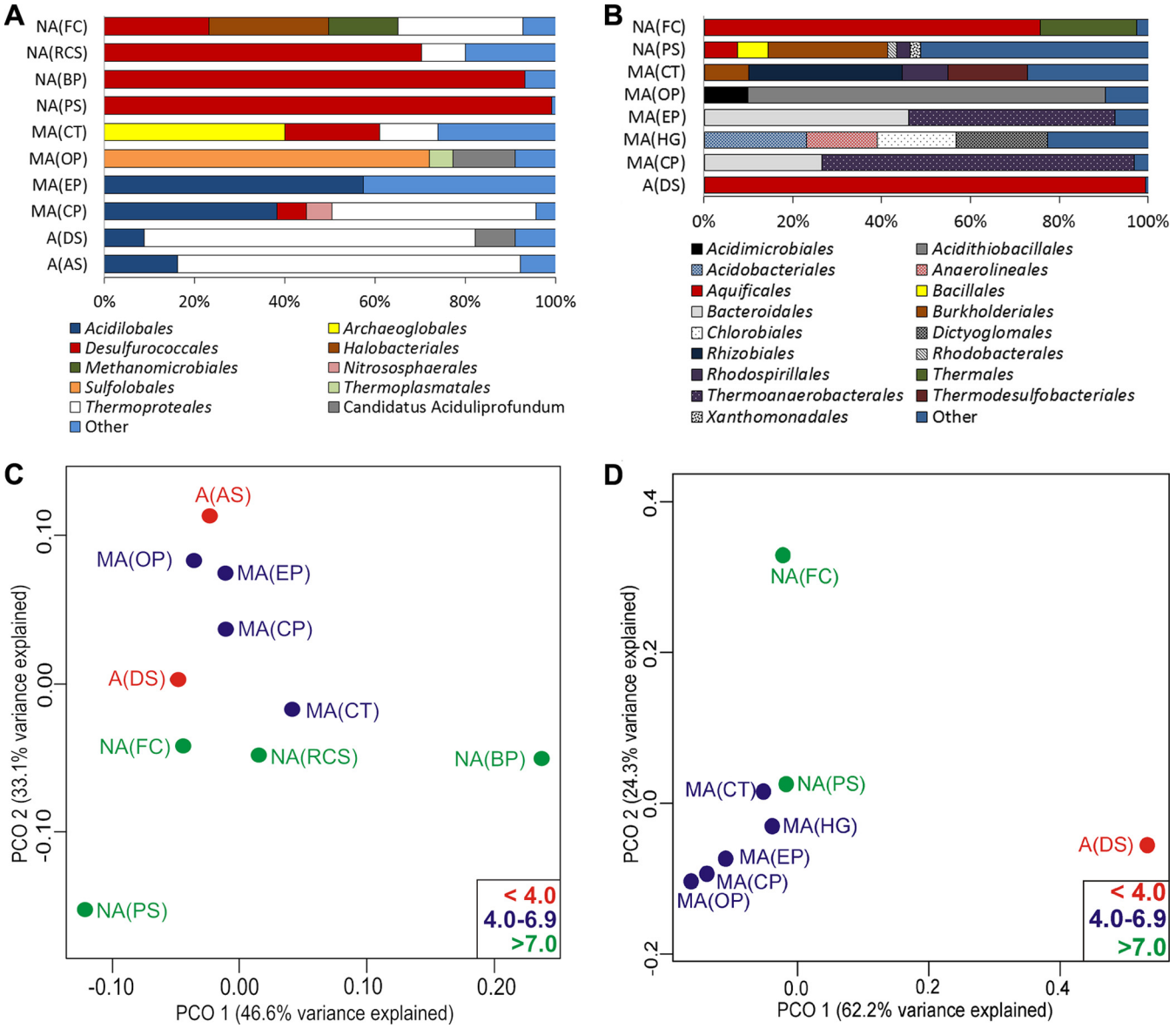

FIG 6 (A and B) Compositions of archaeal (A) and bacterial (B) 16S rRNA genes in DNA extracted from sediments sampled from the sources of the hot springs listed in Tables 1 and 2. (C and D) PCO ordination of the Rao phylogenetic dissimilarity associated with archaeal (C) and bacterial (D) 16S rRNA gene assemblages. Red, acidic springs (pH <4.0); navy blue, moderately acidic springs (pH 4.0 to 6.9); green, neutral to alkaline springs (pH >7.0).

extracts from 8 of the 13 springs, and archaeal amplicons were obtained from sediment DNA extracts from 10 of the 13 springs.

(i) *Archaea.* Following normalization, a total of 1,008 archaeal 16S rRNA gene sequences belonging to 562 distinct OTUs (defined at 3.0% sequence dissimilarities) were identified in the 10 hot spring communities where amplicons were obtained (Fig. 6A). Rarefaction analysis indicated that between 84.6 and 99.8% of the predicted 16S rRNA gene diversity was sampled at this depth of sequencing in these 10 communities (data not shown). Principle coordinates (PCO) analysis was used to identify relationships between archaeal community composition, environmental characteristics, and carbon transformation activities (Fig. 6C). Both the acidic to slightly acidic hot springs A(AS), MA(EP), MA(CP), A(DS), and MA(OP) and the alkaline hot springs NA(RCS) and NA(FC) formed clusters, indicating similar community compositions in hot springs with similar geochemistries. PCO axis 1 (44.6% of variance explained) was not significantly correlated with any of the environmental variables measured. However, this axis was significantly correlated with the rate of DIC assimilation (Pearson $R = 0.92$, $P < 0.01$), acetate assimilation (Pearson $R = 0.76$, $P = 0.01$), and acetate mineralization (Pearson $R = 0.69$, $P = 0.03$) (see Table S3 in the supplemental material). PCO axis 2 (23.7% of variance explained) was significantly correlated with spring pH (Pearson $R = 0.77$, $P < 0.01$), which helps to explain the overall pattern of clustering based on pH.

The relative abundance of a number of the 20 most abundant OTUs varied significantly with rates of substrate transformation (see Table S4 in the supplemental material). The abundances of Otu0001 (*Ignisphaera aggregans*; 94% sequence identities) and Otu0018 (*I. aggregans*; 90% sequence identities) were positively

correlated with the rate of DIC assimilation (Pearson $R = 0.91$ for both), acetate assimilation (Pearson $R = 0.81$ and 0.87, respectively), and acetate mineralization (Pearson $R = 0.76$ and 0.82, respectively). The relative abundances of Otu0005 (*Acidilobus sulfurireducens*; 95% sequence identities), Otu0014 (*Caldisphaera draconis*; 99% sequence identities), and Otu0015 (*Thermogladius shockii*; 98% sequence identities) exhibited strongly positive correlations with the rate of formate mineralization (Pearson $R = 0.86$, 0.78, and 0.86, respectively) and low or inverse correlations with the rate of formate assimilation (Pearson $R = 0.01$, -0.15, and -0.10, respectively). In contrast, the relative abundance of Otu0017 (*Geoglobus acetivorans*; 93% sequence identities) exhibited a strong correlation with the rate of formate assimilation (Pearson $R = 0.80$) but no correlation with the rate of formate mineralization (Pearson $R = 0.01$).

(ii) *Bacteria*. Following normalization, a total of 656 bacterial 16S rRNA gene sequences belonging to 389 distinct OTUs (defined at 3.0% sequence dissimilarities) were identified in the 8 hot spring communities where amplicons were obtained (Fig. 6B). Rarefaction analysis indicated that between 87.9 and 99.8% of the predicted 16S rRNA gene diversity was sampled at this depth of sequencing in these 9 communities (data not shown). PCO analysis was used to identify relationships between bacterial community composition, environmental characteristics, and carbon transformation activities (Fig. 6D). Communities inhabiting the acidic hot spring A(DS) clustered distinctly with respect to those from a cluster comprising the slightly acidic hot springs MA(CT), MA(HG), MA(EP), MA(CP), and MA(OP). The pattern of clustering in A(DS) was driven by the dominance of sequences affiliated with *Hydrogenobaculum* sp. strain NOR3L3B, which was rarely identified in the other springs. In contrast, the community inhabiting the circumneutral hot spring NA(PS) and the alkaline hot spring NA(FC) did not form a cluster. PCO axis 1 (62.2% of variance explained) was significantly correlated with the rate of acetate mineralization (Pearson $R = 0.94$, $P < 0.01$) and with the concentrations of sulfide (Pearson $R = 0.90$, $P < 0.01$), ferrous iron (Pearson $R = 0.89$, $P < 0.01$), and nitrate (Pearson $R = 0.74$, $P = 0.03$) (see Table S6 in the supplemental material). PCO axis 2 (24.3% of variance explained) was significantly correlated with the rate of acetate assimilation (Pearson $R = 0.95$, $P < 0.01$), hot spring pH (Pearson $R = 0.72$, $P = 0.05$), and the concentration of DIC (Pearson $R = 0.76$, $P = 0.03$).

Linear regression indicated significant or strong relationships between the relative abundance of a number of the 20 most abundant bacterial OTUs and rates of individual substrate transformation (see Table S5 in the supplemental material). The relative abundance of Otu0002 (*Thermodesulfobium narugense* Na82; 98% sequence identities) exhibited a strong, positive correlation with the concentration of DIC (Pearson $R = 0.60$, $P = 0.12$). The rate of formate assimilation was significantly correlated with the relative abundance of Otu0017 (*Methylobacterium* sp. strain A4; 96% sequence identities; Pearson $R = 0.98$, $P < 0.01$) and the relative abundance of Otu0020 (*Geothermobacterium ferrireducens* FW-1a; 99% sequence identities; Pearson $R = 0.98$, $P < 0.01$), while the rate of formate mineralization was significantly correlated with the relative abundance of Otu0004 (*Paludibacter propionicigenes* WB4; 93% sequence identities; Pearson $R = 0.90$, $P < 0.12$). The rate of acetate assimilation was significantly correlated with the relative abundance of Otu0005 (*Thermocrinis* sp. strain P2L2B; 98% sequence identities; Pearson $R = 1.00$, $P < 0.01$) and the relative abundance of Otu0011 (*Thermus aquaticus*; 99% sequence identities; Pearson $R = 1.00$, $P < 0.01$), while the rate of acetate mineralization was significantly correlated with the relative abundance of Otu0001 (*Hydrogenobaculum* sp. NOR3L3B; 99% sequence identities; Pearson $R = 0.93$, $P < 0.01$).

DISCUSSION

Molecular and thermodynamic data suggest that nonphotosynthetic microbial communities inhabiting high-temperature (>73°C) hot springs are supported by chemolithoautotrophic metabolism (6, 8, 11, 40, 41). The higher rates of C assimilation from DIC than from the common heterotrophic substrates formate and acetate in the majority of the hot springs examined herein provide the first empirical evidence supporting these predictions and indicate that autotrophic metabolism may predominate in high-temperature geothermal communities. However, the generalization that all communities of this type are supported by chemoautotrophic metabolism is not supported by our data since the rates of C assimilation from formate and acetate were found to exceed those from DIC in 2 of 13 hot spring communities [A(AS) and MA(HG)]. Similar findings indicating a greater extent of labeling of lipids by amendment with organic acid substrates than by amendment with bicarbonate in two alkaline hot springs in YNP (20, 25) further substantiate the claim that organic carbon may play an important and previously overlooked role in supporting these communities.

Individual rates of formate and acetate utilization generally exhibited an inverse correlation with the concentrations of these substrates in the environment, suggesting a potential role for biological activity in depleting these organic acid pools. A previous study documented the assimilation of DIC, formate, acetate, and glucose in two alkaline hot spring communities (20). Incorporation of DIC and organic substrates into the same diagnostic lipids suggested that the populations assimilating these substrates may be facultatively autotrophic. It is also possible that these populations may be capable of the simultaneous utilization of these substrates (mixotrophic), although the experimental design in the aforementioned study did not allow testing of this possibility. A facultatively autotrophic phenotype for the dominant autotrophic populations is supported by the rapid (<45-min) suppression of DIC assimilation observed herein in the presence of low (micromolar) concentrations of formate. This would allow populations to take advantage of the temporally abrupt input of exogenous organic materials from surrounding areas (e.g., by aeolian deposition or through surface runoff from precipitation). Such an explanation is consistent with the findings of a previous compound-specific isotopic analysis of lipid carbon in biomass sampled from several alkaline hot springs in YNP over a period of several years which revealed evidence for a shift between autotrophic and heterotrophic metabolisms in several aquificae biomarker lipids (20, 25). The potential for the input of exogenous organic materials from surrounding areas is also supported by the recovery of bacterial 16S rRNA genes from several of the chemosynthetic communities studied herein [MA(CP), MA(EP), MA(CT), NA(PS), and NA(BP)] that were closely affiliated with orders (*Enterobacteriales*, *Bacteroidales*, *Rhizobiales*, and *Burkholderiales*) that are typically associated with feces-contaminated waters, soils, or root nodules (42–44). Intriguingly, some of the highest rates of organic acid assimilation and mineralization were observed in springs in which sequences

affiliated with these lineages were present. This result is consistent with a recent input of exogenous organic material in these springs.

The suppression of DIC assimilation in the presence of formate could also be attributed to formate dehydrogenase (FDH)-promoted isotopic exchange between [^{12}C]formate and $^{12}CO_2$ or to the production of $^{12}CO_2$ as the product of formate oxidation by a separate population of heterotrophic organisms. Either of these scenarios would, in effect, dilute the spring water DIC pool, resulting in a smaller ratio of ^{14}C-labeled DIC to unlabeled DIC and thus an apparent decrease in the rate of DIC assimilation. However, if the suppression of DIC assimilation was due to dilution of the labeled DIC pool by either of these mechanisms, it would also be expected that the quantity of formate required to achieve the observed suppression would closely match the factor by which the [^{14}C]bicarbonate pool had been diluted by [^{12}C]bicarbonate from oxidized formate. In all environments assayed, the concentration of DIC was at a minimum 125-fold greater than that of formate, indicating that isotopic exchange could account for <0.08% suppression of activity. This strongly indicates that the observed suppression is not due to isotopic exchange.

The low concentrations of ^{14}C-labeled formate and acetate radiotracers used in our microcosm assays were chosen to closely match previously reported concentrations of formate (acetate concentrations have yet to be reported) in YNP hot springs (<10 μM) (18) and thus minimize the rate of induction of microbial processes above their basal or *in situ* rate. Moreover, formate occurs increasingly in the protonated form as pH decreases (it has a pK_a of 3.75 at 80°C, meaning that half of all formate is protonated at pH 3.75). This neutral form readily diffuses into the cell and deprotonates at the intracellular pH, thereby decreasing the membrane potential (45). Previous studies have shown that concentrations of formate as low as 100 μM inhibit the growth of the acidophile *Thiobacillus* (*Acidithiobacillus*) *ferrooxidans* when grown in medium with a pH of 1.6 (46). Since the highest concentration of formate that has been measured in YNP hot springs to date is 10 μM (18) and since several of the springs subject to study have pHs of <3.75 (Table 1), we attempted to avoid the confounding effects of formate toxicity by amending the assay mixtures with <20 μM formate. In addition, to avoid potential error resulting from a low substrate concentration in our calculations of the K_m of formate conversion, we used the equations of Wright and Hobbie, which allow the more accurate calculation of kinetic parameters at low substrate concentrations (e.g., <20 μM) or when the natural substrate concentration is not known (29).

The concentrations of formate and acetate in spring waters sampled from our study sites at the time of our microcosm incubations were lower than anticipated and often were below the detection limit (Table 2). Consequently, the final concentrations of radiolabeled formate and acetate in our microcosm assays were higher than the native concentrations of these substrates in most cases. Since formate and acetate transformation rates were calculated using native concentrations or the detection limit concentration for those substrates, these rates can be considered to reflect upper limits. As a result, the formate and acetate assimilation and mineralization activities reported here may be more appropriately referred to as rate potentials rather than absolute rates. A further consideration which is supported by repeated sampling of hot springs over seasonal or annual cycles is that the concentrations of organic substrates vary temporally (25, 47). This variability makes the estimation of representative substrate transformation rates more difficult and potentially less meaningful, as these rates likely vary to a large degree in accordance with variations in the mode and magnitude of delivery of organic substrates to these systems.

The cumulative rate of measured activities (DIC, formate, and acetate mineralization and assimilation) and the individual rates of C assimilation from DIC, formate, and acetate were generally higher in circumneutral to alkaline low-temperature springs than acidic high-temperature springs. Low rates of metabolic activity or productivity would be expected to translate to lower biomass abundances in acidic high-temperature hot springs than alkaline hot springs. ATP has been used as a measure of biomass in a number of environmental systems (e.g., see reference 48), including hot springs. Atkinson et al. reported ATP concentrations 3 to 4 order of magnitude lower in hot spring sediments sampled from low-pH environments than those sampled from high-pH environments (49). This result would be consistent with the low metabolic activities that are reported here for acidic hot spring communities. Alternatively, considering that not all ATP in a cell is directed toward the production of biomass but, rather, can also be directed toward maintenance functions (50), higher rates of catabolic reactions than anabolic reactions might be required under acidic and high-temperature conditions to counteract the energetic stress imposed on cells from their surrounding environment (51), perhaps leading to lower biomass production. While Atkinson et al. (49) reported only ATP contents and not ATP/ADP ratios, previous studies indicate that the cellular abundance of ATP and the ATP/ADP ratio vary by less than an order of magnitude in *Escherichia coli* cells during various stages of growth and when cells are grown under different metabolic regimes (52). Thus, the variation in ATP contents in hot springs observed by Atkinson et al. (49) is unlikely to be due solely to potential differences in the metabolic state or stress levels of the cells in acidic versus circumneutral to alkaline springs and instead is interpreted to reflect differences in biomass levels in these springs.

The use of 1-[^{14}C]- and 2-[^{14}C]acetate labels (with labeling at the carboxyl and methyl groups, respectively) in microcosm assays provided an opportunity to examine potential differences in the metabolic state of acetate-utilizing populations. Entry of acetate in the form of acetyl coenzyme A (acetyl-CoA) into the tricarboxylic acid (TCA) cycle should result in a higher rate of CO_2 release from the carbonyl carbon of acetyl-CoA (the carboxyl group of acetate), since this carbon is retained only through the first turn of the TCA cycle and is completely lost as CO_2 during the second turn of the cycle. In contrast, the methyl group of acetyl-CoA (the methyl group of acetate) is retained through the first two turns of the TCA cycle and is lost as CO_2 only in the third and fourth turns of the cycle. Siphoning off of TCA cycle intermediates for use in amino acid and lipid biosynthesis would lead to higher rates of assimilation than oxidation. In contrast, cells that are energy limited might maximize the oxidation of acetate, leading to higher levels of NADH/reduced flavin adenine dinucleotide ($FADH_2$) production and the release of acetate carbon as CO_2. The rate of CO_2 production from the methyl and carboxyl carbons of acetate was greater than the rate of CO_2 assimilation in both NA(RCS) and MA(EP), while the rates of assimilation of the methyl and carboxyl carbon positions of acetate were higher than the rates of release of acetate carbon as CO_2 in NA(FC), A(AS), and MA(OP). This suggests that acetate-utilizing cells comprising the communities in NA(RCS) and MA(EP) may be, on average, in a more energy-limited state than cells comprising the communi-

ties in NA(FC), A(AS), and MA(OP), which appear to be in a state of active biosynthesis. Eight of the 13 communities exhibited rates of CO_2 production from the carboxyl carbon of acetate that exceeded the rates of CO_2 production from the methyl group, which would be consistent for the oxidation of acetate via TCA cycle enzymes if this pathway were the primary mechanism for acetate metabolism in these communities. Four of the remaining 5 communities exhibited rates of CO_2 production from the methyl carbon that were statistically significantly indistinguishable from or very similar to the rates of CO_2 production from the carboxyl carbon, which may be attributable to the full oxidation of acetate via the TCA cycle (>4 turns). However, a single community, A(AS), exhibited a rate of CO_2 production from the methyl position of acetate that exceeded that from the carboxyl position. Acetate metabolism in this community is not easily explained by any of the known mechanisms.

The physiology inferred from a number of archaeal and bacterial 16S rRNA gene sequences recovered from the 13 hot spring communities examined was consistent with their potential role in the transformation of DIC, formate, and acetate. For example, the relative abundance of sequences affiliated with *Thermodesulfobium narugense*, a thermophilic and autotrophic sulfate-reducing bacterium (53), was positively correlated with the rate of DIC assimilation. Likewise, the relative abundances of sequences affiliated with several crenarchaeotes, including *A. sulfurireducens* and *C. draconis*, and the euryarchaeote *G. acetivorans* were positively correlated with the rate of formate mineralization. *G. acetivorans*, an iron-reducing facultative chemolithoautotroph, has been shown to be capable of using formate as an electron donor (54). While a cultivation-based study of *A. sulfurireducens* 18D70 and *C. draconis* 18U65 did not reveal the ability to grow via formate oxidation at a formate concentration of 5 mM (32), the partial genome of *A. sulfurireducens* (locus tags Asul_00004590 and Asul_00004590) and the complete genomes of the closely related strains *Acidilobus saccharovorans* 345-15 (locus tags ASAC_0614 and ASAC_0615) and *Caldisphaera lagunensis* IC-154 (locus tags Calag_1200 and Calag_1201) encode homologs of archaeal FDH enzymes (data not shown). The rate of acetate transformation was positively correlated with the relative abundance of the aquificae *Thermocrinis* sp. P2L2B and *T. aquaticus*. Several characterized strains of *Thermocrinis* (7, 14, 15) and the type strain of *T. aquaticus* (55) have been shown to use acetate, consistent with the prevalence of these sequences in springs with high rates of acetate metabolism.

In summary, the results presented here substantiate previous suggestions (6–8, 10, 40, 41) for the importance of chemolithoautotrophy in sustaining high-temperature, nonphotosynthetic hot spring communities. However, the rates of carbon assimilation from the limited array of organic substrates tested here (formate and acetate), in some cases, exceed the rate of assimilation of DIC, suggesting that nonphototrophic communities in hot springs may be reliant on or able to take advantage of organic carbon to support their metabolism. These findings are consistent with recent work by Schubotz et al. (20, 25), which documented the assimilation of organic substrates into lipid biomarkers in two hot spring communities. In support of the potential for facultative autotrophy in spring populations, amendment with successively higher concentrations of formate was found to systematically suppress DIC assimilation. This indicates that organics not only are usable but also may be actively selected for use over DIC when both substrates are available. Together, these results indicate an important and previously underestimated role for organic substrates in supporting nonphototrophic communities that inhabit geochemically diverse hot springs in YNP.

ACKNOWLEDGMENTS

This work was supported by NASA Exobiology and Evolutionary Biology award NNX10AT31G (to T.M.H. and E.S.B.) and NSF Partnerships in International Research and Education award PIRE-0968421 (to J.W.P.).

We declare no conflict of interest.

We thank Christie Hendrix and Stacey Gunther from the YNP Center for Resources for assistance in obtaining permits to perform this work.

REFERENCES

1. **Brock TD.** 1967. Micro-organisms adapted to high temperatures. Nature **214:**882–885. http://dx.doi.org/10.1038/214882a0.
2. **Cox A, Shock EL, Havig JR.** 2011. The transition to microbial photosynthesis in hot spring ecosystems. Chem Geol **280:**344–351. http://dx.doi.org/10.1016/j.chemgeo.2010.11.022.
3. **Hamilton TL, Vogl K, Bryant DA, Boyd ES, Peters JW.** 2012. Environmental constraints defining the distribution, composition, and evolution of chlorophototrophs in thermal features of Yellowstone National Park. Geobiology **10:**236–249. http://dx.doi.org/10.1111/j.1472-4669.2011.00296.x.
4. **Boyd E, Fecteau K, Havig J, Shock E, Peters JW.** 2012. Modeling the habitat range of phototrophic microorganisms in Yellowstone National Park: toward the development of a comprehensive fitness landscape. Front Microbiol **3:**221. http://dx.doi.org/10.3389/fmicb.2012.00221.
5. **Boyd ES, Hamilton TL, Spear JR, Lavin M, Peters JW.** 2010. [FeFe]-hydrogenase in Yellowstone National Park: evidence for dispersal limitation and phylogenetic niche conservatism. ISME J **4:**1485–1495. http://dx.doi.org/10.1038/ismej.2010.76.
6. **Spear JR, Walker JJ, McCollom TM, Pace NR.** 2005. Hydrogen and bioenergetics in the Yellowstone geothermal ecosystem. Proc Natl Acad Sci U S A **102:**2555–2560. http://dx.doi.org/10.1073/pnas.0409574102.
7. **Reysenbach A-L, Banta A, Civello S, Daly J, Mitchel K, Lalonde S, Konhauser K, Rodman A, Rusterholtz K, Takacs-Vesbach C.** 2005. *Aquificales* in Yellowstone National Park, p 129–142. *In* Inskeep WP, McDermott TR (ed), Geothermal biology and geochemistry in Yellowstone National Park. Montana State University, Bozeman, MT.
8. **Meyer-Dombard DR, Shock EL, Amend JP.** 2005. Archaeal and bacterial communities in geochemically diverse hot springs of Yellowstone National Park. Geobiology **3:**211–227. http://dx.doi.org/10.1111/j.1472-4669.2005.00052.x.
9. **Takacs-Vesbach C, Inskeep WP, Jay ZJ, Herrgard MJ, Rusch DB, Tringe SG, Kozubal MA, Hamamura N, Macur RE, Fouke BW, Reysenbach A-L, McDermott TR, Jennings RD, Hengartner NW, Xie G.** 2013. Metagenome sequence analysis of filamentous microbial communities obtained from geochemically distinct geothermal channels reveals specialization of three *Aquificales* lineages. Front Microbiol **4:**84. http://dx.doi.org/10.3389/fmicb.2013.00084.
10. **D'Imperio S, Lehr CR, Oduro H, Druschel G, Kühl M, McDermott TR.** 2008. Relative importance of H_2 and H_2S as energy sources for primary production in geothermal springs. Appl Environ Microbiol **74:**5802–5808. http://dx.doi.org/10.1128/AEM.00852-08.
11. **Boyd ES, Leavitt WD, Geesey GG.** 2009. CO_2 uptake and fixation by a thermoacidophilic microbial community attached to precipitated sulfur in a geothermal spring. Appl Environ Microbiol **75:**4289–4296. http://dx.doi.org/10.1128/AEM.02751-08.
12. **Takai K, Hirayama H, Sakihama Y, Inagaki F, Yamato Y, Horikoshi K.** 2002. Isolation and metabolic characteristics of previously uncultured members of the order *Aquificales* in a subsurface gold mine. Appl Environ Microbiol **68:**3046–3054. http://dx.doi.org/10.1128/AEM.68.6.3046-3054.2002.
13. **Vetriani C, Speck MD, Ellor SV, Lutz RA, Starovoytov V.** 2004. *Thermovibrio ammonificans* sp. nov., a thermophilic, chemolithotrophic, nitrate-ammonifying bacterium from deep-sea hydrothermal vents. Int J Syst Evol Microbiol **54:**175–181. http://dx.doi.org/10.1099/ijs.0.02781-0.
14. **Huber R, Eder W, Heldwein S, Wanner G, Huber H, Rachel R, Stetter KO.** 1998. *Thermocrinis ruber* gen. nov., sp. nov., a pink-filament-forming hyperthermophilic bacterium isolated from Yellowstone National Park. Appl Environ Microbiol **64:**3576–3583.

15. **Eder W, Huber R.** 2002. New isolates and physiological properties of the *Aquificales* and description of *Thermocrinis albus* sp. nov. Extremophiles **6:**309–318. http://dx.doi.org/10.1007/s00792-001-0259-y.
16. **Lang SQ, Butterfield DA, Schulte M, Kelley DS, Lilley MD.** 2010. Elevated concentrations of formate, acetate and dissolved organic carbon found at the Lost City hydrothermal field. Geochim Cosmochim Acta **74:**941–952. http://dx.doi.org/10.1016/j.gca.2009.10.045.
17. **Martens CS, Albert DB, Chanton JP, Pauly GG, Canuel EA.** 1998. Organic acids and light hydrocarbons in hydrothermally altered Guaymas Basin sediments, p A296. Abstr Geol Soc Am Annu Meet.
18. **Windman T, Zolotova N, Schwandner F, Shock EL.** 2007. Formate as an energy source for microbial metabolism in chemosynthetic zones of hydrothermal ecosystems. Astrobiology **7:**873–890. http://dx.doi.org/10.1089/ast.2007.0127.
19. **Kim YJ, Lee HS, Kim ES, Bae SS, Lim JK, Matsumi R, Lebedinsky AV, Sokolova TG, Kozhevnikova DA, Cha S-S, Kim S-J, Kwon KK, Imanaka T, Atomi H, Bonch-Osmolovskaya EA, Lee J-H, Kang SG.** 2010. Formate-driven growth coupled with H_2 production. Nature **467:**352–355. http://dx.doi.org/10.1038/nature09375.
20. **Schubotz F, Hays LE, Meyer-Dombard DAR, Gillespie A, Shock E, Summons RE.** 2015. Stable isotope labeling confirms mixotrophic nature of streamer biofilm communities at alkaline hot springs. Front Microbiol **6:**42. http://dx.doi.org/10.3389/fmicb.2015.00042.
21. **Murphy CN, Dodsworth JA, Babbitt AB, Hedlund BP.** 2013. Community microrespirometry and molecular analyses reveal a diverse energy economy in Great Boiling Spring and Sandy's Spring West in the U.S. Great Basin. Appl Environ Microbiol **79:**3306–3310. http://dx.doi.org/10.1128/AEM.00139-13.
22. **Hügler M, Huber H, Molyneaux SJ, Vetriani C, Sievert SM.** 2007. Autotrophic CO_2 fixation via the reductive tricarboxylic acid cycle in different lineages within the phylum Aquificae: evidence for two ways of citrate cleavage. Environ Microbiol **9:**81–92. http://dx.doi.org/10.1111/j.1462-2920.2006.01118.x.
23. **Reysenbach AL, Wickham GS, Pace NR.** 1994. Phylogenetic analysis of the hyperthermophilic pink filament community in Octopus Spring, Yellowstone National Park. Appl Environ Microbiol **60:**2113–2119.
24. **Jahnke LL, Eder W, Huber R, Hope JM, Hinrichs K-U, Hayes JM, Des Marais DJ, Cady SL, Summons RE.** 2001. Signature lipids and stable carbon isotope analyses of Octopus Spring hyperthermophilic communities compared with those of Aquificales representatives. Appl Environ Microbiol **67:**5179–5189. http://dx.doi.org/10.1128/AEM.67.11.5179-5189.2001.
25. **Schubotz F, Meyer-Dombard DR, Bradley AS, Fredricks HF, Hinrichs KU, Shock EL, Summons RE.** 2013. Spatial and temporal variability of biomarkers and microbial diversity reveal metabolic and community flexibility in streamer biofilm communities in the Lower Geyser Basin, Yellowstone National Park. Geobiology **11:**549–569. http://dx.doi.org/10.1111/gbi.12051.
26. **Holloway JM, Nordstrom DK, Böhlke JK, McCleskey RB, Ball JW.** 2011. Ammonium in thermal waters of Yellowstone National Park: processes affecting speciation and isotope fractionation. Geochim Cosmochim Acta **75:**4611–4636. http://dx.doi.org/10.1016/j.gca.2011.05.036.
27. **Albert DB, Martens CS.** 1997. Determination of low-molecular-weight organic acid concentrations in seawater and pore-water samples via HPLC. Mar Chem **56:**27–37. http://dx.doi.org/10.1016/S0304-4203(96)00083-7.
28. **Hansen T, Gardeler B, Matthiessen B.** 2013. Technical note: precise quantitative measurements of total dissolved inorganic carbon from small amounts of seawater using a gas chromatographic system. Biogeosciences **10:**6601–6608. http://dx.doi.org/10.5194/bg-10-6601-2013.
29. **Wright RR, Hobbie JE.** 1966. Use of glucose and acetate by bacteria and algae in aquatic ecosystems. Ecology **47:**447–464. http://dx.doi.org/10.2307/1932984.
30. **Lizotte MP, Sharp TR, Priscu JC.** 1996. Phytoplankton dynamics in the stratified water column of Lake Bonney, Antarctica. I. Biomass and productivity during the winter-spring transition. Polar Biol **16:**155–162.
31. **Havig JR, Raymond J, Meyer-Dombard DR, Zolotova N, Shock EL.** 2011. Merging isotopes and community genomics in a siliceous sinter-depositing hot spring. J Geophys Res **116:**G1. http://dx.doi.org/10.1029/2010JG001415.
32. **Boyd ES, Jackson RA, Encarnacion G, Zahn JA, Beard T, Leavitt WD, Pi Y, Zhang CL, Pearson A, Geesey GG.** 2007. Isolation, characterization, and ecology of sulfur-respiring crenarchaea inhabiting acid-sulfate-chloride-containing geothermal springs in Yellowstone National Park. Appl Environ Microbiol **73:**6669–6677. http://dx.doi.org/10.1128/AEM.01321-07.
33. **Hamilton TL, Peters JW, Skidmore ML, Boyd ES.** 2013. Molecular evidence for an active endogenous microbiome beneath glacial ice. ISME J **7:**1402–1412. http://dx.doi.org/10.1038/ismej.2013.31.
34. **Schloss PD, Westcott SL, Ryabin T, Hall JR, Hartmann M, Hollister EB, Lesniewski RA, Oakley BB, Parks DH, Robinson CJ.** 2009. Introducing mothur: open-source, platform-independent, community-supported software for describing and comparing microbial communities. Appl Environ Microbiol **75:**7537–7541. http://dx.doi.org/10.1128/AEM.01541-09.
35. **Anisimova M, Gascuel O.** 2006. Approximate likelihood-ratio test for branches: a fast, accurate, and powerful alternative. Syst Biol **55:**539–552. http://dx.doi.org/10.1080/10635150600755453.
36. **Posada D.** 2006. ModelTest server: a web-based tool for the statistical selection of models of nucleotide substitution online. Nucleic Acids Res **34:**W700–W703. http://dx.doi.org/10.1093/nar/gkl042.
37. **Swofford DL.** 2001. PAUP: phylogenetic analysis using parsimony (and other methods), 4.0b10 ed. Sinauer Associates, Sunderland, MA.
38. **Webb CO, Ackerly DD, Kembel SW.** 2008. Phylocom: software for the analysis of phylogenetic community structure and trait evolution. Bioinformatics **24:**2098–2100. http://dx.doi.org/10.1093/bioinformatics/btn358.
39. **Hammer Ø, Harper DAT, Ryan PD.** 2001. PAST: paleontological statistics software package for education and data analysis. Paleontol. Electonica **4**.
40. **Inskeep WP, Ackerman GG, Taylor WP, Kozubal M, Korf S, Macur RE.** 2005. On the energetics of chemolithotrophy in nonequilibrium systems: case studies of geothermal springs in Yellowstone National Park. Geobiology **3:**297–317. http://dx.doi.org/10.1111/j.1472-4669.2006.00059.x.
41. **Shock EL, Holland M, Meyer-Dombard D, Amend JP, Osburn GR, Fischer TP.** 2010. Quantifying inorganic sources of geochemical energy in hydrothermal ecosystems, Yellowstone National Park, USA. Geochim Cosmochim Acta **74:**4005–4043. http://dx.doi.org/10.1016/j.gca.2009.08.036.
42. **Dick LK, Bernhard AE, Brodeur TJ, Santo Domingo JW, Simpson JM, Walters SP, Field KG.** 2005. Host distributions of uncultivated fecal bacteroidales bacteria reveal genetic markers for fecal source identification. Appl Environ Microbiol **71:**3184–3191. http://dx.doi.org/10.1128/AEM.71.6.3184-3191.2005.
43. **Walters SP, Gannon VPJ, Field KG.** 2007. Detection of *Bacteroidales* fecal indicators and the zoonotic pathogens *E. coli* O157:H7, *Salmonella*, and *Campylobacter* in river water. Environ Sci Technol **41:**1856–1862. http://dx.doi.org/10.1021/es0620989.
44. **Rivas R, Velázquez E, Willems A, Vizcaíno N, Subba-Rao NS, Mateos PF, Gillis M, Dazzo FB, Martínez-Molina E.** 2002. A new species of *Devosia* that forms a unique nitrogen-fixing root-nodule symbiosis with the aquatic legume *Neptunia natans* (L.f.) Druce. Appl Environ Microbiol **68:**5217–5222. http://dx.doi.org/10.1128/AEM.68.11.5217-5222.2002.
45. **Russell J.** 1992. Another explanation for the toxicity of fermentation acids at low pH: anion accumulation versus uncoupling. J Appl Bacteriol **73:**363–370. http://dx.doi.org/10.1111/j.1365-2672.1992.tb04990.x.
46. **Pronk JT, Meijer WM, Hazeu W, van Dijken JP, Bos P, Kuenen JG.** 1991. Growth of *Thiobacillus ferrooxidans* on formic acid. Appl Environ Microbiol **57:**2057–2062.
47. **Briggs BR, Brodie EL, Tom LM, Dong H, Jiang H, Huang Q, Wang S, Hou W, Wu G, Huang L, Hedlund BP, Zhang C, Dijkstra P, Hungate BA.** 2014. Seasonal patterns in microbial communities inhabiting the hot springs of Tengchong, Yunnan Province, China. Environ Microbiol **16:**1579–1591. http://dx.doi.org/10.1111/1462-2920.12311.
48. **Jenkinson DS.** 1988. Determination of microbial biomass carbon and nitrogen in soil, p 368–386. *In* Wilson JR (ed), Advances in nitrogen cycling in agricultural ecosystems. CAB International, Wallingford, United Kingdom.
49. **Atkinson T, Cairns S, Cowan DA, Danson MJ, Hough DW, Johnson DB, Norris PR, Raven N, Robinson C, Robson R, Sharp RJ.** 2000. A microbiological survey of Montserrat Island hydrothermal biotopes. Extremophiles **4:**305–313. http://dx.doi.org/10.1007/s007920070018.
50. **Russell JB, Cook GM.** 1995. Energetics of bacterial growth: balance of anabolic and catabolic reactions. Microbiol Rev **59:**48–62.

51. **Valentine DL.** 2007. Adaptations to energy stress dictate the ecology and evolution of the Archaea. Nat Rev Microbiol **5:**316–323. http://dx.doi.org/10.1038/nrmicro1619.
52. **Tran QH, Unden G.** 1998. Changes in the proton potential and the cellular energetics of *Escherichia coli* during growth by aerobic and anaerobic respiration or by fermentation. Eur J Biochem **251:**538–543. http://dx.doi.org/10.1046/j.1432-1327.1998.2510538.x.
53. **Mori K, Kim H, Kakegawa T, Hanada S.** 2003. A novel lineage of sulfate-reducing microorganisms: Thermodesulfobiaceae fam. nov., *Thermodesulfobium narugense*, gen. nov., sp. nov., a new thermophilic isolate from a hot spring. Extremophiles **7:**283–290. http://dx.doi.org/10.1007/s00792-003-0320-0.
54. **Slobodkina GB, Kolganova TV, Querellou J, Bonch-Osmolovskaya EA, Slobodkin AI.** 2009. *Geoglobus acetivorans* sp. nov., an iron(III)-reducing archaeon from a deep-sea hydrothermal vent. Int J Syst Evol Microbiol **59:**2880–2883. http://dx.doi.org/10.1099/ijs.0.011080-0.
55. **Degryse E, Glansdorff N.** 1981. Studies on the central metabolism of *Thermus aquaticus*, an extreme thermophilic bacterium: anapierotic reactions and their regulation. Arch Microbiol **129:**173–177. http://dx.doi.org/10.1007/BF00455357.